# Temperature effects on carrier formation dynamics in organic heterojunction solar cell

Kouhei Yonezawa, Takeshi Yasuda, and Yutaka Moritomo

Citation: Applied Physics Letters **107**, 133903 (2015); doi: 10.1063/1.4932375
View online: http://dx.doi.org/10.1063/1.4932375
View Table of Contents: http://scitation.aip.org/content/aip/journal/apl/107/13?ver=pdfcov
Published by the AIP Publishing



# Temperature effects on carrier formation dynamics in organic heterojunction solar cell

Kouhei Yonezawa,[1] Takeshi Yasuda,[2] and Yutaka Moritomo[1,3,a)]
[1]*Graduate School of Pure and Applied Science, University of Tsukuba, Tsukuba 305-8571, Japan*
[2]*Photovoltaic Materials Unit, National Institute for Materials Science (NIMS), Tsukuba 305-0047, Japan*
[3]*Center for Integrated Research in Fundamental Science and Engineering (CiRfSE), University of Tsukuba, Tsukuba 305-8571, Japan*

(Received 4 August 2015; accepted 23 September 2015; published online 2 October 2015)

The femto-second time-resolved spectroscopy was performed on the heterojunction (HJ) solar cell which consists of prototypical low-band gap donor (D), poly[[4,8-bis[(2-ethylhexyl)oxy]benzo[1,2-*b*:4,5-*b*′] dithiophene-2,6-diyl][3-fluoro-2-[(2-ethylhexyl)carbonyl]thieno[3,4-*b*] thiophenediyl]] (PTB7), and the $C_{70}$ acceptor (A). We spectroscopically determined the absolute number of donor exciton ($n_{D*}$), acceptor exciton ($n_{A*}$), and carrier ($n_{D+}$) per an absorbed photon against the delay time ($t$). At 300 K, we found that the decay time ($\tau_{decay} = 3.5$ ps) of A* is much longer than the carrier formation time ($\tau_{form} = 1.1$ ps), indicating that the late A* component does not contribute to the carrier formation process. The elongated $\tau_{form}$ (=1.5 ps) at 80 K is ascribed to the exciton migration process, not to the exciton dissociation process. © *2015 AIP Publishing LLC*.
[http://dx.doi.org/10.1063/1.4932375]

Organic solar cells (OSCs) with bulk heterojunction (BHJ)[1,2] are promising energy conversion devices with flexibility and low-cost production process, e.g., the roll-to-roll process. The BHJ active layer, which is usually sandwiched between an indium tin oxide (ITO) transparent anode and an Al cathode, consists of phase-separated nano domains of the donor (D) polymers and acceptor (A) molecules. The OSC realizes the light-to-electric energy conversion by the combination of the carrier formation and the transfer processes. In the carrier formation process, the photo-irradiation creates the excitons within the nano domains. The excitons migrate to the D/A interface and are dissociated into electron and hole across the interface. In the carrier transfer process, the electron and hole transfer to the cathode and anode, respectively. This is in a sharp contrast with the inorganic solar cells (ISCs), in which the photo-irradiation directly creates the free carriers within the active layer.

The development of low-band gap donor polymers, e.g., PTB7, increases the power conversion efficiency (PCE) of OSCs in the last decade.[3,4] The increase in the PCE stimulates extensive spectroscopic investigations of the low-band gap blend films.[5–9] Recently, several experiments[10–15] revealed nanostructure of the BHJ active layer. The scanning transmission x-ray microscopy (STXM) around the carbon K-edge revealed fullerene mixing within the polymer–rich domain.[10–13] In addition, by means of atomic force microscopy (AFM) coupled with plasma-ashing technique, Hedley *et al.*[14] found that the polymer matrix (100–200 nm) of PTB7/$PC_{71}BM$ blend film consists of a large number of small fullerene spheres (20–60 nm). Such a nano-scale domain structure is essential for the efficient carrier formation process, because the exciton migration distance is very short (∼3 nm).

The complexity of the BHJ domain structure, however, has prevented a true understanding of the charge formation process. In this sense, a planer heterojunction (HJ) solar cell with well-defined D/A interface is appropriate for detailed investigation on the carrier formation dynamics. Devizis *et al.*[16] probed the electric field against the delay time ($t$) in the HJ solar cell which consists of 2,2,3,3-tetrafluoropropanol of trimethine cyanide dye with $PF_6^-$ (Cy3-P) and $C_{60}$. They proposed that a weakly bound electron-hole pair at the D/A interface plays a dominant role in the carrier formation process. Takahashi *et al.*[17] investigated carrier injection dynamics in the HJ solar cell with bipolar molecule. We note that spectroscopic investigation of the HJ solar cell is further effective to separate the exciton migration and dissociation processes, because it consists of bulky A and D domains.

In this letter, we spectroscopically determined the absolute number of donor exciton ($n_{D*}$), acceptor exciton ($n_{A*}$), and carrier ($n_{D+}$) per an absorbed photon against $t$ in PTB7/$C_{70}$ HJ solar cell. In these analyses, we determined the coefficient between the photoinduced absorption (PIA) and exciton (carrier) number by the differential (electrochemical differential) spectra of neat film. The temporal evolution of the species indicates that the exciton migration is disadvantageous for the exciton dissociation at the D/A interface. We observed that the exciton migration, not the exciton dissociation, elongates the carrier formation time ($\tau_{form}$) from 1.1 ps at 300 K to 1.5 ps at 80 K.

PTB7/$C_{70}$ HJ solar cell was fabricated with a structure of ITO/poly-(3,4-ethylenedioxythiophene) (PEDOT): poly-(styrenesulfonate) (PSS) (40 nm)/PTB7 (18 nm)/$C_{70}$ (25 nm)/bathocuproine (BCP) (5 nm)/MgAg. The patterned ITO (conductivity: 10/sq) glass was pre-cleaned in an ultrasonic bath of acetone and ethanol and then treated in an ultraviolet-ozone chamber. A thin layer of PEDOT:PSS (40 nm) was spin-coated onto the ITO and dried at 110 °C for 10 min on a hot plate in air. A neat PTB7 film was spin-coated from an

a)Author to whom correspondence should be addressed. Electronic mail: moritomo.yutaka.gf@u.tsukuba.ac.jp

 

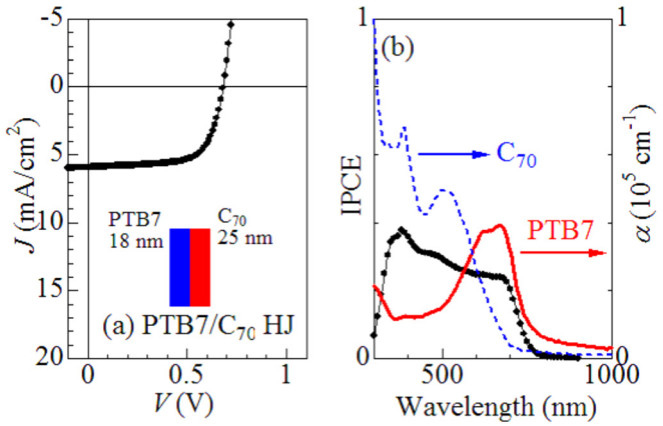


FIG. 1. (a) Current density-voltage ($J$–$V$) curves of PTB7/$PC_{70}BM$ HJ solar cell. (b) Incident photon to current conversion efficiency (IPCE) spectra of the device, together with the absorption coefficients ($\alpha$) of PTB7 and $C_{70}$.

$o$-dichlorobenzene ($o$-DCB) solution. PTB7 was purchased from Sigma-Aldrich and used as received. The AFM image of the PTB7 film is flat and consists of small grains less than 100 nm. Then, $C_{70}$ (25 nm) was deposited by vacuum evaporation. Finally, BCP and MgAg were deposited onto the active layer by conventional thermal evaporation at a chamber pressure lower than $5 \times 10^{-4}$ Pa, which provided the devices with an active area of 2 5 $mm^2$.

Figure 1(a) shows current density-voltage ($J$-$V$) curves of the PTB7/$PC_{70}BM$ HJ solar cell. The curves were measured using a voltage current source/monitor under AM 1.5 solar-simulated light irradiation of 100 $mW/cm^2$ (Bunkou-keiki, OTENTO-SUN III). The HJ device exhibits an open circuit voltage ($V_{oc}$) of 0.68 V, a short circuit current ($J_{sc}$) of 5.9 $mA/cm^2$, a fill factor (FF) of 0.68, and a PCE of 2.7%. Figure 1(b) shows incident photon to current conversion efficiency (IPCE) spectra of the devices, which was measured using a SM-250 system (Bunkou-keiki).

For the time-resolved spectroscopy, PTB7/$C_{70}$ bilayer film was prepared on the quartz substrates. First, PTB7 neat film (18 nm) was spin-coated on quartz substrate from an $o$-DCB solution and was dried in an inert $N_2$ atmosphere. Then, $C_{70}$ (25 nm) was deposited by vacuum evaporation. We further prepare the PTB7 (100 nm) and $C_{70}$ (25 nm) neat films. The time-resolved spectroscopy[9] was carried out in a pump-probe configuration at 300 K and 80 K. The film was placed on a cold head of a cryostat, whose temperature was controlled with a liquid nitrogen. The wavelength of the pump pulse was 400 nm, which is expected to excite both D* and A*. The pulse width and repetition rate are 100 fs and 1000 Hz, respectively. The excitation intensity ($I$) was 27 $\mu J/cm^2$. The spot sizes of the pump and probe pulses were 4.2 and 2.0 mm in diameter, respectively. The transmitted probe spectra were detected using a 256 ch InGaAs photodiode array (800–1600 nm) attached to a 30 cm imaging spectrometer. The differential absorption ($\Delta$OD) spectra is expressed as $\Delta OD \equiv -\log(\frac{I_{on}}{I_{off}})$, where $I_{on}$ and $I_{off}$ are the transmission spectra under the "pump-on" and "pump-off" conditions, respectively.

Figure 2(a) shows $\Delta$OD spectra of the PTB7/$C_{70}$ bilayer film. The spectra shows a broad PIA centered at 1160 nm. The PIA is originated from the photoinduced carriers ($D^+$) on the donor polymer.[5,8,9] Actually, the spectral profile is similar to that of the electrochemical differential absorption spectra of the PTB7 neat film.[21] In the early state (~1 ps), however, we observed additional absorption components around 1500 nm. The additional components are reasonably ascribed to the PIAs due to donor (D*) and acceptor (A*) excitons. Figure 2(b) shows $\Delta$OD spectra of the PTB7 neat film. We observed a characteristic PIA due to D*. Actually, the spectral profile is the same at least up to 10 ps. In the late stage above 100 ps, the profile changes probably due to formation of triplet exciton. Figure 2(c) shows $\Delta$OD spectra of the $C_{70}$ neat film. We observed a flat and weak PIA due to A*.

In order to reveal the carrier formation dynamics, we decomposed the PIA ($\phi_{exp}$) of the PTB7/$C_{70}$ bilayer film into the PIA components due to $D^+$ ($\phi_{D+}$), D* ($\phi_{D*}$), and A* ($\phi_{A*}$). We regarded the $\Delta$OD spectra of the PTB7/$C_{70}$ bilayer (average between 8 and 10 ps), the PTB7 neat (at 1 ps) and $C_{70}$ neat (at 1 ps) films as the basis functions, $\phi_{D+}$, $\phi_{D*}$, and $\phi_{A*}$, respectively. We neglected the long-living photo excited species such as triplet exciton, because they cannot be directly photo created. We do not explicitly include the PIA component due to acceptor electron ($A^-$), because it is included in the $D^+$ component and cannot be separated. The spectral weights, i.e., $C_{D+}$, $C_{D*}$, and $C_{A*}$, of

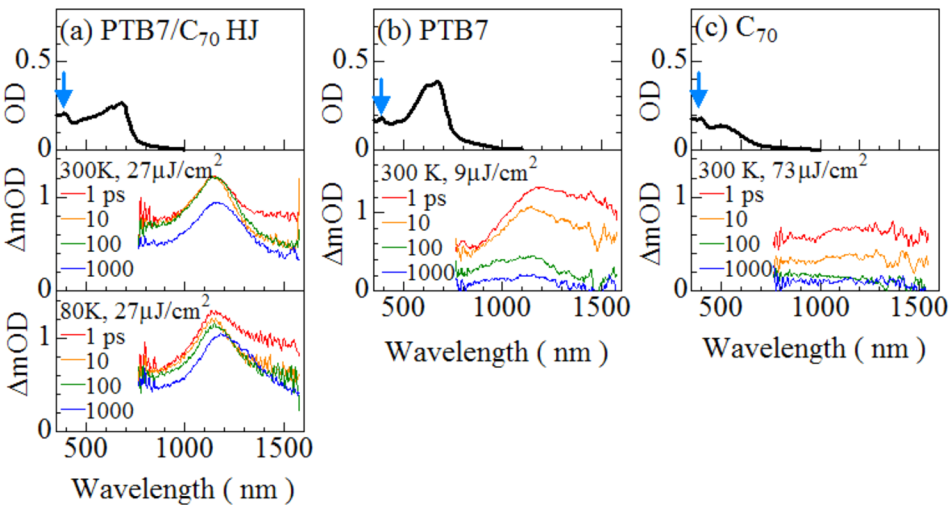


FIG. 2. Differential absorption ($\Delta$OD) spectra of (a) PTB7/$C_{70}$ bilayer, (b) PTB7, (c) $C_{70}$ neat films. Top panels show optical density (OD) of (a) PTB7/$C_{70}$ bilayer, (b) PTB7, and (c) $C_{70}$ neat films.

the respective components were determined so that they minimize the trial function

$$F = \Sigma_i[(C_{D+}\phi_{D+} + C_{D*}\phi_{D*} + C_{A*}\phi_{A*}) - \phi_{exp}]^2. \quad (1)$$

Figure 3(a) shows a prototypical example of the spectral decompositions at 300 K. We clearly observed that the 400 nm excitation excites both D* and A*.

To spectroscopically evaluate the absolute numbers of the carrier ($n_{D+}$), donor exciton ($n_{D*}$), and donor carrier ($n_{A*}$) per an absorbed photon, we need the absolute intensity of the PIAs per unit densities of $D^+$, D*, and A*. By means of the electrochemical differential spectroscopy,[21] the PIA intensity per unit carrier density was determined to be $\alpha_{carrier} = 0.013\,nm^2$/carrier. Then, $n_{D+}$ can be calculated by $\alpha_{photon}/\alpha_{carrier}$, where $\alpha_{photon}$ is the PIA intensity of the $D^+$ component per unit photon density. To determine the PIA intensities per unit exciton densities, we assumed that one absorbed photon creates one D* (A*) in the PTB7 ($C_{70}$) neat film. Then, the PIA intensity per unit density of D* (A*) becomes $\alpha_{exciton} = 0.020$ (0.001) $nm^2$/exciton with considering absorption index. Then, $n_{D*}$ ($n_{A*}$) can be calculated by $\alpha_{photon}/\alpha_{exciton}$, where $\alpha_{photon}$ is the PIA intensity of the D* (A*) component per unit photon density.

In Fig. 3(c), we plotted thus obtained $n_{D+}$, $n_{D*}$, and $n_{A*}$ against $t$ at 300 K. We plotted adjacent averages in $n_{A*}$, because the $n_{A*}$ values significantly scatter due to the small coefficient ($\alpha_{exciton} = 0.001\,nm^2$/exciton). The solid curves are results of least-squares fittings with exponential functions. The obtained characteristic times ($\tau_{form}$ and $\tau_{decay}$) and amplitudes ($C$) for $D^+$, D*, and A* are listed in Table I.

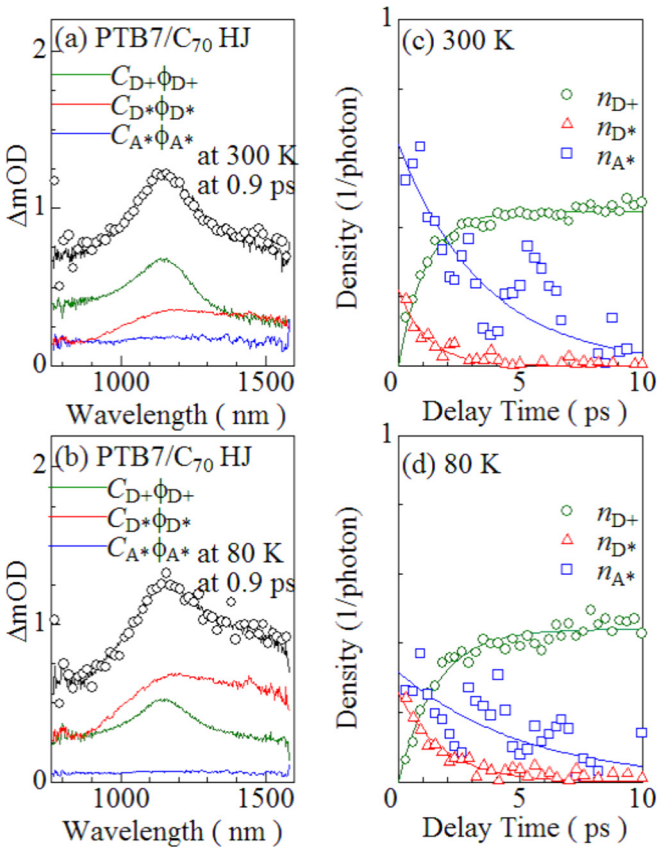


FIG. 3. ΔOD spectra (open circles) of PTB7/$C_{70}$ bilayer film at (a) 300 K and (b) 80 K, together with the spectral decomposition into PIAs due to $D^+$ ($C_{D+}\phi_{D+}$), D* ($C_{D*}\phi_{D*}$), and A* ($C_{A*}\phi_{A*}$). Absolute number of carrier ($n_{D+}$), donor exciton ($n_{D*}$), and acceptor exciton ($n_{A*}$) per an absorbed photon against the delay time at (c) 300 K and (d) 80 K. Adjacent averages were plotted in $n_{A*}$. The solid curves in (c) and (d) are results of the least-squares fittings with exponential functions.

TABLE I. Characteristic times ($\tau_{form}$ and $\tau_{decay}$) and amplitudes ($C$) of $n_{D+}$, $n_{D*}$, and $n_{A*}$. The parameters were obtained by least-squares fittings with exponential function: $C\times(1-e^{-\frac{t}{\tau_{form}}})$ for $n_{D+}$ and $C\times e^{-\frac{t}{\tau_{decay}}}$ for $n_{D*}$ and $n_{A*}$.

| Species | Temperature (K) | $\tau_{form}$ (ps) | $\tau_{decay}$ (ps) | $C$ (1/photon) |
|---|---|---|---|---|
| $D^+$ | 300 | 1.1 | … | 0.45 |
| $D^+$ | 80 | 1.5 | … | 0.44 |
| D* | 300 | … | 1.2 | 0.22 |
| D* | 80 | … | 1.8 | 0.26 |
| A* | 300 | … | 3.5 | 0.64 |
| A* | 80 | … | 5.1 | 0.32 |

Our careful analysis revealed that $\tau_{decay}$ (=3.5 ps) of A* is longer than $\tau_{form}$ (=1.1 ps). This indicates that the late A* component (≥1 ps) does not contribute to the carrier formation process. Consistently, the sum (=0.86 exciton/photon) of the initial exciton number is larger than the final carrier number (=0.44 carrier/photon). In other words, exciton dissociation efficiency steeply decreases with $t$. This is probably because late A* component has no excess energy[18] enough to separate into electron and hole across the D/A interface. Such a hot exciton picture is theoretically supported.[19,20] On the other hand, $\tau_{decay}$ (=1.2 ps) of D* is comparable with $\tau_{form}$ (=1.1 ps), indicating that the exciton dissociation efficiency remains high. This is probably because the excess energy of D* is much higher than that of A* at 400 nm excitation.

Now, let us proceed to the temperature effects on the carrier formation process. Figure 3(d) shows $n_{D+}$, $n_{D*}$, and $n_{A*}$ against the delay time at 80 K. $\tau_{form}$ and $\tau_{decay}$ elongate at 80 K: 1.5 ps (1.1 ps) for $D^+$, 1.8 ps (1.2 ps) for D*, and 5.1 ps (3.5 ps) for A* at 80 K (300 K). The exciton-to-carrier conversion process can be divided into two processes, i.e., the exciton migration to the D/A interface and exciton dissociation across the interface. We know that $\tau_{form}$ of the PTB7/$PC_{71}BM$ BHJ solar cell is 0.2–0.3 ps,[9] which is the longer limit of the exciton dissociation time, Then, in the PTB7/$C_{70}$ HJ solar cell at 300 K, the exciton migration time is longer than 0.8–0.9 ps while the exciton dissociation time is shorter than 0.2–0.3 ps. In other words, $\tau_{form}$ of the HJ device is dominated by the exciton migration process. Therefore, the elongation of $\tau_{form}$ at 80 K should be ascribed to the slow exciton migration.

Finally, let us discuss the electron-hole recombination process in the late stage. At the early state after the carrier formation, the carriers are considered to be localized in the vicinity of the D/A interface.[16] Figures 4(a) and 4(b) show the ΔOD spectra of PTB7/$C_{70}$ bilayer film at 300 K and 80 K, respectively. The observed red-shift of the PIA peak is ascribed to energy relaxation of the carriers due to polaron formation or relaxation within density of state. At 300 K, the energy relaxation of $D^+$ saturates at ~500 ps

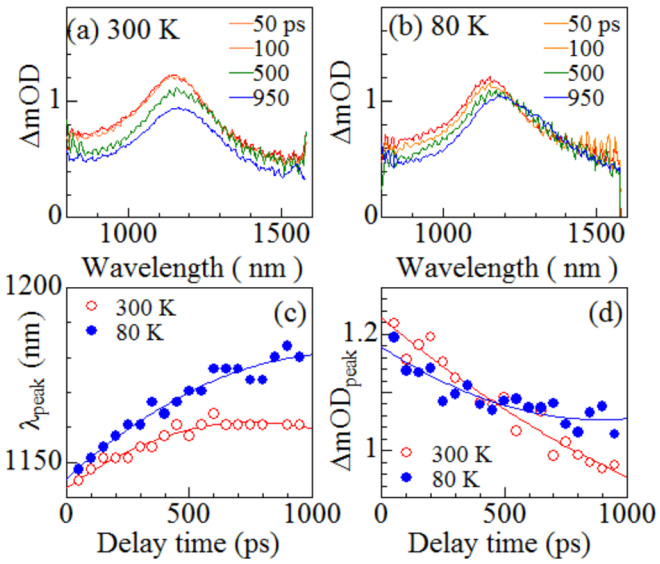


FIG. 4. ΔOD spectra of PTB7/$C_{70}$ bilayer film at (a) 300 K and (b) 80 K. (c) Peak wavelength ($\lambda_{peak}$) and (d) peak intensity ($\Delta OD_{peak}$) against delay time. The solid curves in (c) and (d) are merely the guide to the eyes.

[Fig. 4(c)]. The resultant mobile nature causes rapid decease in $\Delta OD_{peak}$ [Fig. 4(d)] mediated by the electron-hole recombination. We note that high excitation pulse energy causes the high carrier density ($N_{DA}$) at the D/A interface. The high $N_{DA}$ is partly responsible for the rapid decreases in $\Delta OD_{peak}$, because the recombination probability is proportional to $N_{DA}^2$. Actually, the internal quantum efficiency ($\phi_{IQ}$) of the regioregular poly(3-hexylthiophene) (rr-P3HT)/PCBM BHJ solar cell steeply decreases with excitation pulse energy.[21] At 80 K, the energy relaxation becomes steeper than that at 300 K [Fig. 4(c)]. Then, the resultant carrier localization[22] suppresses the electron-hole recombination process [Fig. 4(d)].

In conclusion, we spectroscopically determined on the absolute numbers of $D^+$, D*, and A* against $t$ in PTB7/$C_{70}$ HJ solar cell and clarified the temperature effects on them. The quantitative analyses enable us to separate the exciton migration and dissociation processes. We found that exciton migration is disadvantageous for the exciton dissociation at the D/A interface. The observation is interpreted in terms of the hot exciton picture. We further found that the exciton migration, not the exciton dissociation, elongates $\tau_{form}$ form 1.1 ps at 300 K to 1.5 ps at 80 K.

This work was supported by Futaba Electronics Memorial Foundation.

[1]M. Hiramoto, H. Fujiwara, and M. Yokoyama, Appl. Phys. Lett. **58**, 1062 (1991).
[2]N. S. Sariciftci, L. Samilowitz, A. H. Heeger, and F. Wudl, Science **258**, 1474 (1992).
[3]Y. Liang, Z. Xu, J. Xia, S.-T. Tsai, Y. Wu, G. Li, C. Ray, and L. Yu, Adv. Energy Mater. **22**, E135 (2010).
[4]Z. He, C. Zhong, S. Su, M. Xu, H. Wu, and Y. Cao, Nat. Photonics **6**, 593 (2012).
[5]J. Guo, Y. Liang, J. Szarko, B. Lee, H.-J. Son, B. S. Rolczynski, L. Yu, and L. X. Chen, J. Phys. Chem. B **114**, 742 (2010).
[6]J. M. Szarko, J.-C. Guo, B. S. Rolczynski, and L. X. Chen, J. Mater. Chem. **21**, 7849 (2011).
[7]B. S. Rolczynski, J. M. Szarko, H. J. Son, Y. Liang, L. Yu, and L. X. Chen, J. Am. Chem. Soc. **134**, 4142 (2012).
[8]K. Yonezawa, H. Kamioka, T. Yasuda, L. Han, and Y. Moritomo, Appl. Phys. Express **5**, 042302 (2012).
[9]K. Yonezawa, H. Kamioka, T. Yasuda, L. Han, and Y. Moritomo, Jpn. J. Appl. Phys., Part 1 **52**, 062405 (2013).
[10]B. A. Collins, Z. Li, J. R. Tumbleston, R. Gann, C. R. McNeill, and H. Ade, Adv. Energy Mater. **3**, 65 (2013).
[11]W. Ma, J. R. Tumbleston, M. Wang, E. Gann, F. Huang, and H. Ade, Adv. Energy Mater. **3**, 864 (2013).
[12]Y. Moritomo, T. Sakurai1, T. Yasuda, Y. Takeichi, K. Yonezawa, H. Kamioka, H. Suga, Y. Takahashi, Y. Yoshida, N. Inami *et al*., Appl. Phys. Express **7**, 052302 (2014).
[13]Y. Moritomo, T. Yasuda, K. Yonezawa, T. Sakurai, Y. Takeichi, H. Suga, Y. Takahashi, N. Inami, K. Mase, and K. Ono, Sci. Rep. **5**, 9483 (2015).
[14]G. J. Hedley, A. J. Ward, A. Alekseev, C. T. Howells, E. R. Martins, L. A. Serrano, G. Cooke, A. Ruseckas, and I. D. W. Samuel, Nat. Commun. **4**, 2867 (2013).
[15]S. V. Kesava, Z. Fei, A. D. Rimshaw, C. Wang, A. Hexemer, J. B. Asbury, M. Heeney, and E. D. Gomez, Adv. Energy Mater. **4**, 1400116 (2014).
[16]A. Devizis, J. D. Jonghe-Risse, R. Hany, F. Nüesch, S. Jenatsch, V. Gulbinas, and J.-E. Moser, J. Am. Chem. Soc. **137**, 8192 (2015).
[17]Y. Takahashi, T. Yasuda, K. Yonezawa, and Y. Moritomo, Appl. Phys. Lett. **106**, 123902 (2015).
[18]S. D. Dimitrov, A. A. Bakulin, C. B. Nielsen, B. C. Schroeder, J. Du, H. Bronstein, I. McCulloch, R. H. Friend, and J. R. Durrant, J. Am. Chem. Soc. **134**, 18189 (2012).
[19]H. Tamura and I. Burghardt, J. Am. Chem. Soc. **135**, 16364 (2013).
[20]M. Huix-Rotllant, H. Tamura, and I. Burghardt, Phys. Chem. Lett. **6**, 1702 (2015).
[21]Y. Moritomo, K. Yonezawa, and T. Yasuda, Appl. Phys. Lett. **105**, 073902 (2014).
[22]A. Deviszis, K. Meerholz, D. Hertel, and V. Gulbinas, Phys. Rev. B **82**, 155204 (2010).